UDC 621.365.5 **doi: 10.20998/2074-272X.2018.1.05**

V.M. Zolotaryov, M.A. Shcherba, R.V. Belyanin, R.P. Mygushchenko, O.Yu. Kropachek

COMPARATIVE ANALYSIS OF ELECTRICAL AND THERMAL CONTROL OF THE LINING STATE OF INDUCTION APPARATUS OF COPPER WIRE MANUFACTURE

Aim. ***This article is intended to develop a technique for monitoring the lining state of induction channel furnaces for melting oxygen-free copper by monitoring changes in the distribution of thermal fields in their lining and carrying out a comparative analysis of the developed technique with the existing one that controls the electrical resistance of the melting channel of the furnaces.*** ***Technique.*** ***For carrying out the research, the theories of electromagnetic field, thermodynamics, mathematical physics, mathematical modeling based on the finite element method were used.*** ***Results.*** ***A technique for diagnosing the lining state of the induction channel furnaces for melting oxygen-free copper has been developed, which makes it possible to determine the dislocation and the size of the liquid metal leaks by analyzing the temperature distribution over the body surface both the inductor and the furnace.*** ***Scientific novelty.*** ***The connection between the temperature field distribution on the surface of the furnace body and the dislocation and dimensions of the liquid metal leaks in its lining is determined for the first time.*** ***Practical significance.*** ***Using the proposed technique will allow to conduct more accurate diagnostics of the lining conditions of the induction channel furnaces, as well as to determine the location and size of the liquid metal leaks, creating the basis for predicting the working life of the furnace.*** References 10, tables 3, figures 4.

Key words: **induction heating, diagnostics and control, interconnected electromagnetic and thermal processes, thermal field distribution, three-dimensional mathematical modeling, finite element method.**

Цель. ***Целью статьи является разработка методики контроля состояния футеровки индукционных канальных печей для плавки бескислородной меди путем мониторинга изменений распределения тепловых полей в их футеровке и проведение сравнительного анализа разработанной методики с существующей, которая контролирует электрическое сопротивление плавильного канала печей.*** ***Методика.*** ***Для проведения исследований использовались положения теории электромагнитного поля, термодинамики, математической физики, математического моделирования с применением метода конечных элементов.*** ***Результаты.*** ***Разработана методика диагностики состояния футеровки индукционной канальной печи для плавки бескислородной меди, которая позволяет определять дислокацию и размер протеканий жидкого металла путем анализа распределения температуры по поверхности корпуса индуктора и печи.*** ***Научная новизна.*** ***Впервые установлена связь между распределением температурного поля на поверхности корпуса печи и дислокацией и размерами протеканий жидкого металла в ее футеровке.*** ***Практическое значение.*** ***Использование предложенной методики позволит проводить более точную диагностику состояния футеровки индукционных канальных печей, а также определять расположение и размеры протеканий жидкого металла, создавая основы для прогнозирования ресурса работы печи.*** Библ. 10, табл. 3, рис. 4.

Ключевые слова: **индукционный нагрев, диагностика и контроль, взаимосвязанные электромагнитные и тепловые процессы, распределение теплового поля, трехмерное математическое моделирование, метод конечных элементов.**

Introduction. Taking into account the constant increase in energy prices and imported components of industrial induction apparatus, the urgency of increasing their resource and energy efficiency, as well as import substitution of the component equipment, is increasing. [3, 8]. All these tasks need to be addressed during the melting of ultrapure oxygen-free copper in induction channel furnaces, in particular in the UPCAST furnaces [6], the application of which is expanded due to a number of technological advantages.

The resource of the UPCAST induction channel furnaces depends on the duration of the failure-free operation of the inductor, which heats the liquid metal channel (0.3 tons), and the furnace, which is above the inductor and contains most of the liquid melt (up to 10 tons). At present, there is a problem of matching the resources of the inductor and the furnace. If the predicted working life of the furnace is 4-6 years, then working life of the inductor is only 1-2 years, i.e. the technology includes a planned 2-3-fold replacement of the inductor design with unchanged furnace design [6, 10].

However, joint experimental studies of PJSC Yuzhcable Works (Kharkiv) and the Institute of Electrodynamics of the National Academy of Sciences of Ukraine (Kiev) using UPCAST line US20X-10 as an example on the continuous casting of oxygen-free copper wire have showed that the replacement procedure of the inductor significantly reduces the working life of the furnace [8]. Due to the temperature drop from 1150 °C (the temperature of the copper melt and the furnace lining surface) up to 300-400 °C (the temperature of furnace lining after the copper draining during its heating with gas burners), the lining inevitably cracks. After re-commissioning the furnace with a new inductor and an old lining, liquid metal leaks occur in cracks.

The most expedient solution to this problem is to increase working life of the inductor to working life of the furnace and use them as a single system during the entire continuous cycle lasting 4-6 years. As a consequence, the line resource is expected to increase beyond 4-6 years due to the lack of planned inductor replacements. The first step to achieve this goal is to improve the system for diagnosing the lining thermal state of the inductor and the furnace.

Now the diagnostics is based on monitoring the active and reactive inductor resistance by measuring the impedance of the melting channel and the water temperature as it passes through the cooling system pipes [6]. The furnace lining is monitored visually and copper leaks through lining are inaccessible for inspection and it

is made by measuring the temperature of the furnace body. This method of diagnostics is indirect, since it does not allow revealing the location and size of the leaks areas of liquid metal, and the actual state of the furnace and inductor is determined by inspection only after they are completely stopped and cooled.

Therefore, there is a need to develop a new technique for diagnosing the lining state, which would allow estimating the direct location and dimensions of the liquid metal leaks into the lining cracks and thus predicting working life of the furnace.

The aim of the paper is to develop a technique for monitoring the lining state of induction channel furnace for melting oxygen-free copper by monitoring changes in the distribution of thermal fields in it using a three-dimensional mathematical model.

Three-dimensional mathematical model. According to the physical formulation, the problem of induction heating of a metal consists of electromagnetic and thermal problems with strong mutual relations [1, 2, 5, 9].

To calculate the distribution of the magnetic field and the current density, the system of Maxwell equations with respect to the vector potential $\vec{A}$ is solved.

$$\mathrm{rot}\vec{H} = \vec{J}, \quad \vec{B} = \mathrm{rot}\vec{A}, \qquad (1, 2)$$

$$\vec{J} = \sigma(T)\vec{E} + \vec{J}_{ext}, \quad \vec{E} = -\mathrm{grad}\varphi - \frac{\partial \vec{A}}{\partial t}, \qquad (3, 4)$$

where $\vec{B}$, $\vec{H}$, $\vec{E}$ are vectors of magnetic induction, magnetic and electric fields intensity, $\vec{J}$, $\vec{J}_{ext}$ are the density vectors of the total current and current in the inductor busbars, φ is the electric scalar potential, σ(T) is electric conductivity of copper, which is a function of temperature T and is described by the following expression:

$$\sigma(T) = \frac{1}{\rho_0(1+\alpha(T-T_{ref}))}, \qquad (5)$$

where $\rho_0 = 1.72\cdot10^{-8}$ Ohm·m is specific electric resistance of copper, $\alpha = 3.9\cdot10^{-8}$ K^{-1} is its temperature resistance coefficient, $T_{ref} = 273.15$ ºK is reference temperature.

The ferromagnetic properties of the magnetic core of the inductor are described by the magnetization curve:

$$\vec{H} = f(B)\vec{B}/B. \qquad (6)$$

The inductor is connected to a 50 Hz sine voltage transformer and consumes from 14 to 616 kW. Simulated processes of continuous heating, especially with primary starts, can last more than 18 hours. Since the scales of the electromagnetic and thermal processes on the time axis differ significantly (20 ms period of electromagnetic oscillations and more than 64,800 with the heating duration), then while solving the general interrelated problem, the electromagnetic subtask is solved in the frequency domain using the actual values for the magnetization curve, and the thermal subtask is solved in the time domain [4].

The calculation equations for various elements of the inductor are:

- for a copper template:

$$\mathrm{rot}\left[\frac{1}{\mu_0}\mathrm{rot}\,\dot{\vec{A}}\right] + j\omega\sigma(T)\dot{\vec{A}} = 0, \qquad (7)$$

- for copper inductor busbars:

$$\mathrm{rot}\left[\frac{1}{\mu_0}\mathrm{rot}\,\dot{\vec{A}}\right] - \dot{\vec{J}}_{ext} = 0, \qquad (8)$$

- for steel core:

$$\mathrm{rot}\left[\frac{1}{\mu_0\mu_{ef}}\mathrm{rot}\,\dot{\vec{A}}\right] = 0, \qquad (9)$$

- for lining mixture, steel casing, water cooling system and ambient air:

$$\mathrm{rot}\left[\frac{1}{\mu_0}\mathrm{rot}\,\dot{\vec{A}}\right] = 0. \qquad (10)$$

The solutions of equation (7) – (10) were joined on the boundaries of the elements and were supplemented by the Dirichlet conditions $\vec{n}\cdot\vec{A} = 0$ on the boundaries of the computational domain.

To calculate the heat distribution, the thermal balance equation is solved:

$$\rho C_p \frac{\partial T}{\partial t} - k\,\Delta T = Q_{eddy} + Q_{water}, \qquad (11)$$

where ρ, C_p, k are density, heat capacity and thermal conductivity of materials, Q_{eddy}, Q_{water} are heat sources, including the heating of the template by eddy currents Q_{eddy} (the time average over one period) and cooling of busbars and lining in the course of water flowing through the tubes of the cooling system Q_{water}.

The heat removal through the water was calculated taking into account the heat capacity of the water, its temperature and the mass flow:

$$Q_{water} = M_t \cdot C_p (T_{in} - T)/V, \qquad (12)$$

where M_t is water flow in kilograms, passing through the cross section of the tubes per unit time, T_{in} is the temperature of incoming water, V is the internal volume of the system pipes.

The multi-physical relationship between the problems of calculating the distributions of magnetic and thermal fields was realized by using the eddy currents as a source of heat induced by the magnetic field and determined according to the solution of the electromagnetic problem:

$$Q_{eddy} = 0.5\cdot\sigma(T)\,|\,\vec{E}\,|^2 = 0.5\cdot\sigma(T)\,|\,\partial\vec{A}/\partial t\,|^2. \qquad (13)$$

Equation (11) was supplemented by conditions on the boundaries of the computational domain and on the boundaries of various materials. The convective heat removal from the inductor and the furnace bodies through the ambient air was determined at a given heat transfer coefficient h according to the equation:

$$-k\frac{\partial T}{\partial n} = h(T - T_{ext}), \qquad (14)$$

where T_{ext} is the ambient temperature, n is the normal vector to the outer boundary.

According to the engineering drawings of the channel furnace used at PJSC Yuzhcable Works, a three-dimensional model was constructed in the software

package Comsol Multiphysics [4], for which the solution of the system of differential equations (7) – (11) was found by the finite elements method.

Comparative analysis of electrical and thermal control. Lining furnace is formed by four layers of brick, where the first and second layers serve as «armor» and keep the metal melt from leaks. In this case, the temperature difference at the boundaries of these layers is 119 °C (from 1150 to 1031 °C). The third and fourth layers perform the functions of the heat insulator and the main temperature drop at 899 °C (from 1031 to 132 °C) occurs on their boundaries [6]. However, because of the porous structure, the third and fourth layers of brick after penetration of the metal melt through the «armor» actively absorb it, which eventually leads to the metal flow to the outer steel body of the furnace. As a result, even drops of liquid copper may appear, emerging through its technological holes. Because of this, areas of high temperature rise appear on the body. Such processes increase the power consumption, i.e. reduce the energy efficiency of the entire production process and significantly reduce working life of the furnace.

At the moment, the diagnostics of its resource is carried out by monitoring and recording the active R and reactive X of the inductor resistance. Fig. 1,*a* shows black dots which are the results of measuring the impedance Z of the melting channel of the inductor at PJSC Yuzhcable Works for the period from 01.2013 to 09.2017.

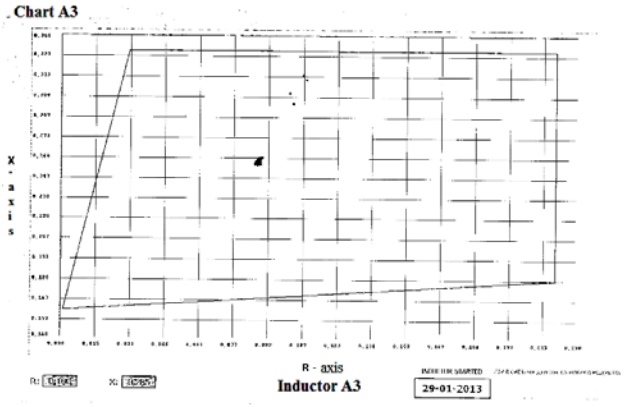

a

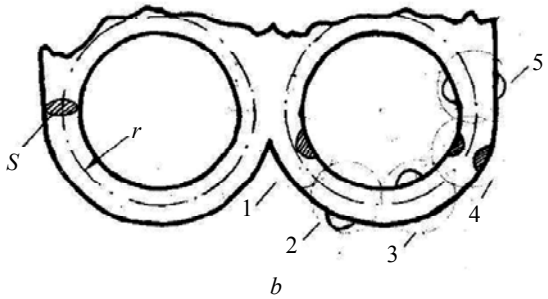

b

Fig. 1. Measurements of impedance Z of the melting channel of the inductor at PJSC Yuzhcable Works (*a*); the shape of the melting channel and its possible defects (*b*)

The active resistivity of the R channel is plotted in ohms along the ordinate axis and its reactive resistance X. The value of R varies inversely with the cross-sectional area of the channel S in Fig. 1,*b* ($R \sim 1/S$). The value X has an inductive character and is proportional to the channel radius ($X \sim r$). The region bounded by the quadrilateral in Fig. 1,*a* is the region of values of the impedance Z of the channel during normal operation of the inductor. The deviation of the measured values of Z beyond the limits of the quadrilateral indicates the emergency operation of the induction apparatus, which is connected with the flow of the melt into the lining of the furnace or vice versa by the entrapment of the melting channel slags in the inductor.

Table 1 shows the change in the parameters R, X, and Z for each of the five types of melting channel defects shown in Fig. 1,*b*.

Table 1

The change of the parameters R, S and Z of the melting channel for each of the five types of its defects

	$R \sim 1/S$	$X \sim r$	Z
1	↑	↑	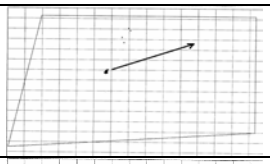
2	↓	↑	
3	↓	↓	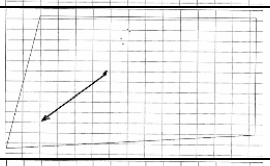
4	↑	unchanged	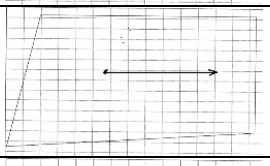
5	↓	unchanged	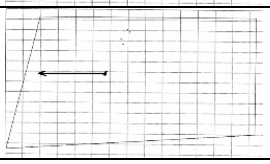

Also, the existing diagnostics system includes monitoring the change in the temperature T of the running water in the cooling system. The system has 4 water-cooled circuits, the tubes of this circuit pass along the surface of the furnace adjoining to the inductor, along the surface of the cylindrical inductor holes for the magnetic circuit, inside the copper busbars and the inductor body base. According to the technical documentation, if the difference in ΔT across all circuits remains within 5 °C, then the line condition is considered normal.

To improve the diagnostics system, it was suggested to monitor not only the system-specific parameters (impedance Z and temperature difference ΔT), but also the temperature distribution along the inductor and furnace bodies. The task was to develop a mathematical model and a technique for calculating the temperature distributions both on the body surface and inside the lining of the inductor and furnace in nominal and emergency operation modes. The verification of the model was carried out by comparing the isotherms

calculated on the body with the real ones measured on the operating casting line.

According to the developed method, with a non-uniform temperature distribution on the surface of the metal casings of the furnace and inductor, temperature changes in local areas and sizes of such areas are monitored. Then, the model determines the shape and size of the melt flowing in the furnace lining and inductor to obtain isotherms that coincide with the experimental ones. With the help of this approach, the instantaneous state of the furnace is diagnosed.

Table 2

The measurement results of the values T_{min}, T_{max} and ΔT in the cathode loading zone

	The cathode loading zone, T_{min}, °C								
	1	2	3	4	5	6	7	8	9
1	70	95	75	78	115	115	70	70	71
2	101	89	105	105	105	105	70	70	56
3	92	96	95	130	124	99	79	79	60
4	70	85	85	95	95	99	80	80	74
	The cathode loading zone, T_{max}, °C								
	1	2	3	4	5	6	7	8	9
1	95	78	77	96	95	95	98	65	95
2	105	90	105	105	105	105	70	69	64
3	105	91	135	152	124	120	79	80	68
4	95	96	91	108	90	88	83	82	79
	The cathode loading zone, ΔT, °C								
	1	2	3	4	5	6	7	8	9
1	25	0	2	18	0	0	1	0	24
2	4	1	0	0	0	0	0	0	8
3	13	5	45	22	0	21	0	1	8
4	25	11	6	13	0	0	3	2	5

Table 3

The measurement results of the values T_{min}, T_{max} and ΔT in the wire drawing zone

	The wire drawing zone, T_{min}, °C								
	1	2	3	4	5	6	7	8	9
1	75	72	77	81	101	87	91	95	95
2	62	62	75	119	119	11	129	118	105
3	71	88	143	127	115	115	128	145	117
4	92	109	124	75	122	120	101	99	71
	The wire drawing zone, T_{max}, °C								
	1	2	3	4	5	6	7	8	9
1	105	105	110	110	102	105	130	110	115
2	106	118	130	226	150	151	160	163	125
3	120	148	242	215	180	190	199	201	141
4	140	200	254	170	202	170	182	154	108
	The wire drawing zone, ΔT, °C								
	1	2	3	4	5	6	7	8	9
1	30	45	33	29	20	18	39	15	5
2	44	56	55	107	31	40	31	45	20
3	49	60	99	88	65	75	71	56	24
4	48	91	130	95	80	50	81	55	37

To predict working life of the furnace, a study was made on the change in the isotherms on the furnace body after a long operating time. An experiment with duration of 3.5 years (from 04.2014 to 09.2017) was planned and conducted to measure the temperature T on the inductor body and the line furnace. The main attention was paid to the furnace, since it contains the bulk of the melt.

The furnace body was divided into 72 control zones (36 in the section for loading copper cathodes for melting and 36 for the stretching of the copper wire), in which the temperature T was measured by an optical pyrometer.

Table 2 for the cathode loading zone and Table 3 for the wire drawing zone show the measurement results of the minimum temperature T_{min} (measured in 2014), the maximum temperature T_{max} (observed from 2014 to 2017) and the temperature difference ΔT reflecting the increase in the average operating temperatures in the zones due to the melt flowing into the lining.

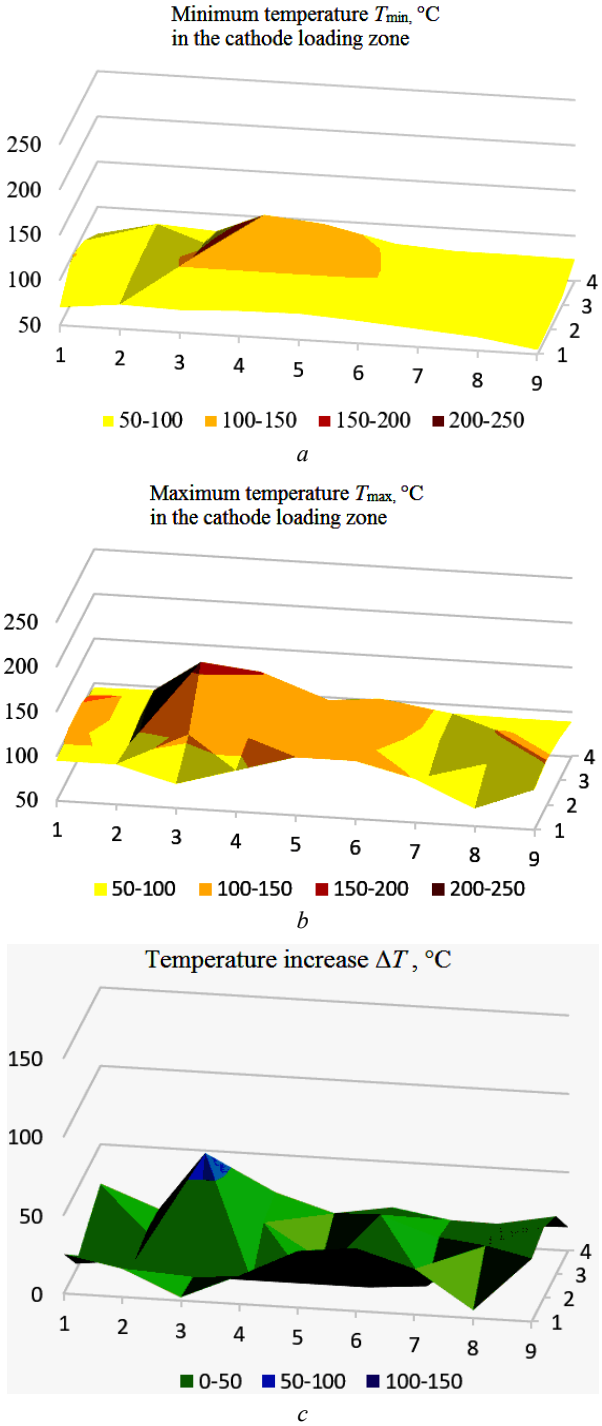

Fig. 2. The measurement results of the values T_{min}, T_{max} and ΔT in the cathode loading zone

The measurement results are plotted accordingly in the diagrams in Fig. 2 and Fig.3, where the height and color of the peaks demonstrate the location and temperature of the zones of the furnace body. Fig. 2,*a* and Fig. 3,*a* show the temperature distribution measurements T_{min} according to measurements made in 2014, when the furnace lining had a small number of defects. Fig. 2,*b* and Fig. 3,*b* show the distribution of the maximum temperature T_{max}, which was observed for 3.5 years of industrial operation of the furnace. Fig. 2,*c* and Fig. 3,*c* reflect the temperature increase over the body ΔT due to the lining degradation.

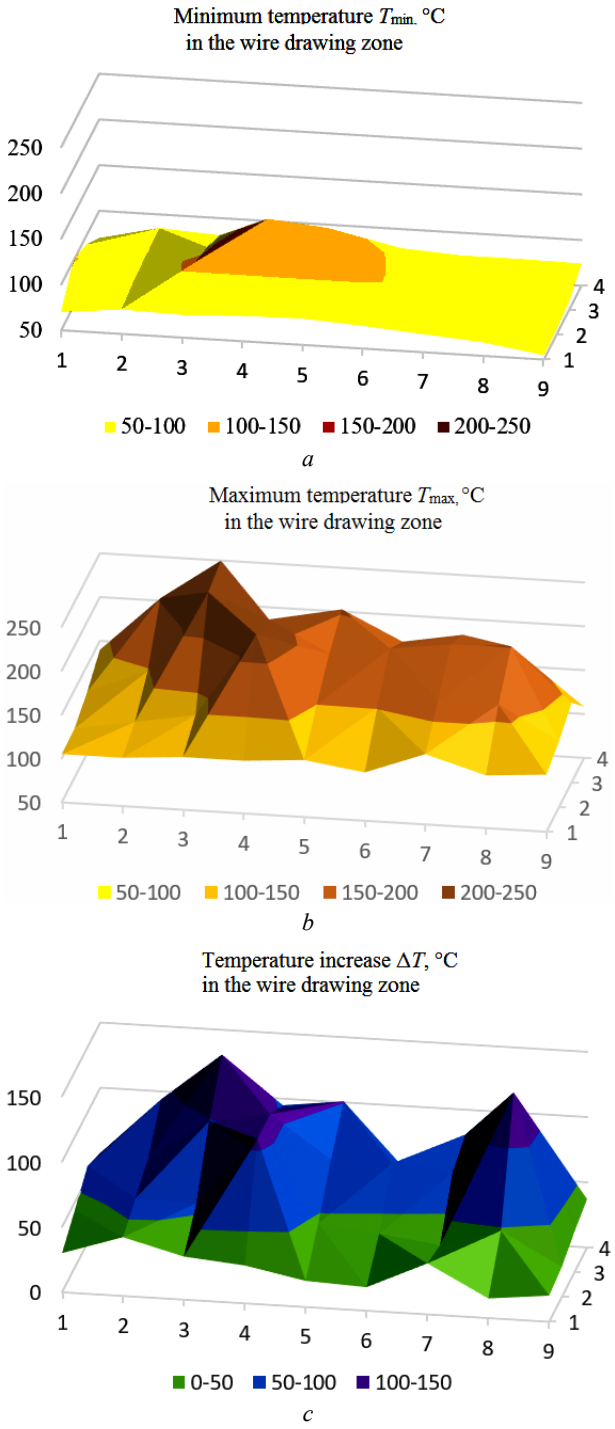

Fig. 3. The measurement results of the values T_{min}, T_{max} and ΔT in the wire drawing zone

Fig. 4 shows graphs of temperature increase T in time in the four hottest control points.

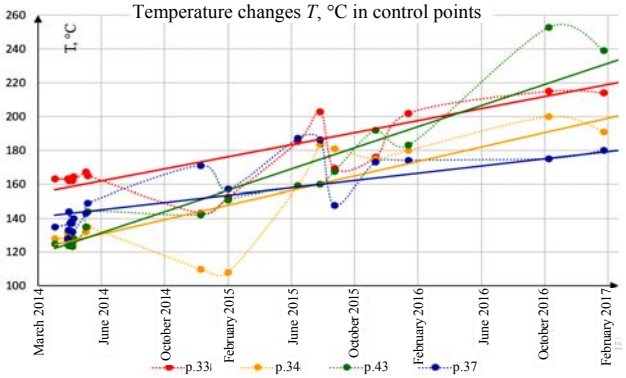

Fig. 4. Temperature increase T in time in the four hottest control zones

Comparing the experimental results in Fig. 2 and Fig. 3, we note that in the wire drawing zone higher temperatures are observed, and this can be seen in both minimum and maximum values. If in the cathode loading zone the average values are $T_{min\ av1}$ = 82 °C and $T_{max\ av1}$ = = 101 °C, then in the wire drawing zone these values are $T_{min\ av2}$ = 96 °C and $T_{max\ av2}$ = 154 °C.

It was determined that during the operation of the furnace, the average temperature on its body increased by 58 °C (from 96 °C to 154 °C). At the same time, in the wire drawing zone, the maximum temperature is 254 °C, as shown by the peak in Fig. 3,*b*, and three zones of the greatest temperature increase (to 130, 107, and 81 °C), which is shown by the three peaks in Fig. 3,*c*. Such an increase in temperature indicates the presence of several zones of liquid metal flowing into the furnace lining and its degradation in the future.

Conclusions.

1. The method of monitoring the lining state of induction channel furnaces for melting oxygen-free copper is well-reasoned by monitoring changes in the distribution of thermal fields in their lining. According to the proposed method, the temperature and location of the hottest areas are measured on the furnace body, according to which, using a three-dimensional mathematical model, the shape and size of the metal melt flowing into the lining is determined.

2. As a result of the planned experiment (lasting 3.5 years) and controlling the change in temperature T in 72 control zones of the furnace casing and inductor of the casting line of the copper wire UPCAST US20X-10 at PJSC Yuzhcable Works, regions of greatest temperature, temperature gradients on the body, and also their variations with time are detected.

3. It was determined that during the operation of the furnace, the average temperature on its body increased by 58 °C (from 96 °C to 154 °C). At the same time, in the wire drawing zone, the maximum temperature was 254 °C, as shown by the peak in Fig. 3b, and three zones of the greatest temperature increase (to 130, 107, and 81 °C), which indicates the presence of several zones leaks in lining furnace

4. The use of the proposed technique allows more accurate diagnostics of the lining state of the induction

channel furnaces, as well as determining the location and size of the liquid metal flow, creating the basis for predicting the working life of the furnace.

REFERENCES

1. .Bermúdez A., Gómez D., Muñiz M.C., Salgado P., Vázquez R. Numerical simulation of a thermo-electromagneto-hydro-dynamic problem in an induction heating furnace. *Applied Numerical Mathematics*, 2009, vol.59, no.9, pp. 2082-2104. **doi: 10.1016/j.apnum.2008.12.005.**

2. Gleim T., Schröder B., Kuhl D. Nonlinear thermo-electromagnetic analysis of inductive heating processes. *Archive of Applied Mechanics*, 2015, vol.85, no.8, pp. 1055-1073. **doi: 10.1007/s00419-014-0968-1.**

3. Lucia O., Maussion P., Dede E.J., Burdio J.M. Induction heating technology and its applications: past developments, current technology, and future challenges. *IEEE Transactions on Industrial Electronics*, 2014, vol.61, no.5, pp. 2509-2520. **doi: 10.1109/TIE.2013.2281162**.

4. Pepper D.W., Heinrich J.C. *The Finite Element Method: Basic Concepts and Applications with MATLAB, MAPLE, and COMSOL*. CRC Press, 2017. 610 p.

5. Stegmueller M.J.R., Schindele P., Grant R.J. Inductive heating effects on friction surfacing of stainless steel onto an aluminum substrate. *Journal of Materials Processing Technology*, 2015, vol.216, pp. 430-439. **doi: 10.1016/j.jmatprotec.2014.10.013**.

6. *UPCAST, Finland*. Available at: http://www.upcast.com (accessed 10 May 2017).

7. Hadad Y., Kochavi E., Levy A. Inductive heating with a stepped diameter crucible. *Applied Thermal Engineering*, 2016, vol.102, pp. 149-157. **doi: 10.1016/j.applthermaleng.2016.03.151**.

8. Zolotaryov V.M., Belyanin R.V., Podoltsev O.D. Analysis of electromagnetic processes in the induction channel furnace used in the cable industry. *Works of the Institute of Electrodynamics of the National Academy of Sciences of Ukraine*, 2016, vol.44, pp. 110-115. (Rus).

9. Shcherba A.A., Podoltsev O.D., Kucheriava I.M., Ushakov V.I. Computer modeling of electrothermal processes and thermo-mechanical stress at induction heating of moving copper ingots. *Technical Electrodynamics*, 2013, no.2, pp. 10-18. (Rus).

10. Zolotaryov V.M., Shcherba M.A., Belyanin R.V. Three-dimensional modeling of electromagnetic and thermal processes of induction melting of copper template with accounting of installation elements design. *Technical Electrodynamics*, 2017, no.3, pp. 13-21. (Rus).

Received 07.11.2017

V.M. Zolotaryov[1]*, Doctor of Technical Science,*
M.A. Shcherba[2]*, Candidate of Technical Science,*
R.V. Belyanin[1]*,*
R.P. Mygushchenko[3]*, Doctor of Technical Science,*
O.Yu. Kropachek[3]*, Candidate of Technical Science,*
[1] Private Joint-stock company Yuzhcable works,
7, Avtogennaya Str., Kharkiv, 61099, Ukraine,
phone +380 57 7545228, e-mail: zavod@yuzhcable.com.ua
[2] The Institute of Electrodynamics of the NAS of Ukraine,
56, prospekt Peremogy, Kiev-57, 03680, Ukraine,
phone +380 44 3662460, e-mail: m.shcherba@gmail.com
[3] National Technical University «Kharkiv Polytechnic Institute»,
2, Kyrpychova Str., Kharkiv, 61002, Ukraine,
phone +380 57 7076116, e-mail: mrp1@ukr.net